Boundary Layer Clouds and Vegetation–Atmosphere Feedbacks

JEFFREY M. FREEDMAN, DAVID R. FITZJARRALD, KATHLEEN E. MOORE, AND RICARDO K. SAKAI

Atmospheric Sciences Research Center, University at Albany, State University of New York, Albany, New York

(Manuscript received 3 September 1999, in final form 31 January 2000)

ABSTRACT

An analysis of boundary layer cumulus clouds and their impact on land surface–atmosphere exchange is presented. Seasonal trends indicate that in response to increasing insolation and sensible heat flux, both the mixed-layer height (z_i) and the lifting condensation level (LCL) peak (~1250 and 1700 m) just before the growing season commences. With the commencement of transpiration, the Bowen ratio falls abruptly in response to the infusion of additional moisture into the boundary layer, and z_i and LCL decrease. By late spring, boundary layer cumulus cloud frequency increases sharply, as the mixed layer approaches a new equilibrium, with z_i and LCL remaining relatively constant (~1100 and 1500 m) through the summer. Boundary layer cloud time fraction peaks during the growing season, reaching values greater than 40% over most of the eastern United States by June. At an Automated Surface Observing System (ASOS) station in central Massachusetts, a growing season peak is apparent during 1995–98 but reveals large variations in monthly frequency due to periods of drought or excessive wetness. Light–cloud cover regression relationships developed from ASOS ceilometer reports for Orange, Massachusetts, and Harvard Forest insolation data show a good linear fit ($r^2 = 0.83$) for overall cloud cover versus insolation, and a reasonable quadratic fit ($r^2 = 0.48$) for cloud cover versus the standard deviation of insolation, which is an indicator of sky type. Diffuse fraction (the ratio of diffuse to global insolation) shows a very good correlation ($r^2 = 0.79$) with cloud cover. The sky type–insolation relationships are then used to analyze the impact that boundary layer clouds have on the forest ecosystem, specifically net carbon uptake (F_{CO_2}), evapotranspiration (ET), and water use efficiency (WUE). During 1995, afternoon F_{CO_2} was 52% greater on days with boundary layer cumulus clouds than on clear days, although ET was the same, indicating greater light use efficiency and WUE on partly cloudy days. For 1996–98, afternoon F_{CO_2} was also enhanced, especially during dry periods. Further analysis indicates that the vapor pressure deficit (VPD) was significantly greater (>8 hPa) during 1995 and parts of 1996–98 on clear days as compared with partly cloudy days. A long-term drought combined with abnormally warm weather likely contributed to the high VPDs, reduced F_{CO_2}, ET, and the dearth of clouds observed during 1995. In general, the presence of boundary layer cumulus clouds enhances net carbon uptake, as compared with clear days.

1. Introduction

Boundary layer cumulus clouds (fair weather nonprecipitating cumulus) play a crucial role in modulating the exchange of radiation, heat, and moisture within and above the planetary boundary layer (Stull 1988). Moreover, the presence of boundary layer cumulus clouds (BLcu) is strongly associated with the type and quantity of underlying vegetation, through this energy exchange. The poor representation of BLcu in numerical weather prediction (Tiedtke 1989, 1993) and global climate models (e.g., Weare et al. 1995), in part due to the transient nature and subgrid spatial scale of small cumulus clouds, produces large prognostic uncertainties in terms of short-term cloud cover forecasts (Jakob 1999). Furthermore, the impact of variable cloud cover on net carbon uptake is not explicitly considered in global atmosphere–biosphere models (Ruimy et al. 1995). Therefore, to better assess the impact BLcu have on surface–atmosphere exchange, a more in-depth analysis of their seasonal frequency, effect on the light environment, and relationship with the heat, moisture, and CO_2 budgets is needed.

BLcu are a daytime and seasonal phenomenon, featuring a distinct diurnal cycle with a seasonal peak in frequency that is coupled with the surface–atmosphere state (see below). Richardson (1922) first hypothesized that the presence of leaves may impact surface–atmosphere exchange processes through the injection of additional moisture into the atmosphere through transpiration. Later observation and modeling studies suggested that forests may be responsible for a large percentage of convective clouds and rainfall in the Tropics (Anthes 1984; Mahfouf et al. 1987; Segal and Arritt 1992; Woodcock 1992; Blyth et al. 1994; Trenberth 1999).

Corresponding author address: Dr. Jeffrey M. Freedman, Atmospheric Information Services, 251 Fuller Road, Albany, NY 12203. E-mail: jmf@atmiserv.com

During the growing season, when the Great Plains and midwestern United States are under the influence of surface high pressure, the distribution of BLcu is coupled with land-cover type and surface moisture (Marotz et al. 1975; Rabin et al. 1990; Carleton et al. 1994; Rabin and Martin 1996; O'Neal 1996). Rabin et al. (1990), using satellite observations from one day in June 1988, showed that during relatively dry conditions, cumulus clouds first formed over a mesoscale-sized (100 km $\times$ 300 km) area of harvested wheat that was adjacent to areas dominated by growing vegetation. Enhancement of cumulus frequency for one month over cleared versus forested areas was also observed by Cutrim et al. (1995) in Amazonia. In contrast with Rabin et al. and Cutrim et al., Carleton et al. (1994) found an increase in convective clouds over forested areas, as compared with cropped areas, in the Midwest during both drought and nondrought summers. O'Neal (1996) found that over central North America, deciduous or coniferous forests have a higher mean convective cloud cover than cropland, especially for weak flow days.

There have been numerous modeling studies analyzing the impact of mesoscale-sized (20–200 km) surface-type inhomogeneities on cloud forcing (e.g., Lynn et al. 1998). These exercises have identified mesoscale or secondary circulations associated with land surface discontinuities, such as dry and wet surfaces (Chen and Avissar 1994), or vegetation–bare ground boundaries (Clark and Arritt 1995). Rabin et al. (1990), however, found that cumulus onset and cloud cover was not simply dependent upon surface type or contrast, but was also a function of the surface energy partition (i.e., Bowen ratio) and mixed-layer stability. Using a surface-energy budget model, they showed that the timing of convection was dependent upon the temperature and moisture profile in the lower atmosphere and landscape characteristics. When the lower atmosphere was relatively moist, convective clouds first developed downwind of moist surface areas. Given a drier atmosphere, cumulus development first occurred over the hotter, drier surface (cf. Chen and Avissar 1994).

Observational studies have speculated that mesoscale circulations are responsible for observed patterns of cumulus convection during quiescent weather conditions (Rabin et al. 1990; Segal and Arritt 1992; Cutrim et al. 1995; Rabin and Martin 1996; Brown and Arnold 1998). However, the actual existence of such secondary or mesoscale circulations in nature has rarely been demonstrated, with the exception of sea, lake, or river breezes (see, e.g., Segal et al. 1997). Such circulations, if detected, have been found to be very weak (Mahrt et al. 1994; Doran et al. 1995). Zhong and Doran (1997) have found that spatial variations in surface temperature and humidity, rather than secondary circulations and resultant mesoscale fluxes, are more influential in determining cloud amount and areas of cloud formation.

Most of the observational studies cited above were limited to the U.S. Great Plains or the Midwest. There have been no observational studies, to date, analyzing the seasonal relationships between BLcu and surface–atmosphere exchange in the northeastern United States. Although the characteristic length scale for typical land-cover features in the northeastern United States is less than 10 km, which Shuttleworth (1991) has classified as disorganized, (or not subject to any organized mesoscale circulations), secondary circulations, such as those related to topography, proximity to large bodies of water, or vegetation, also play a role in determining BLcu onset and cloud frequency.

Monteith (1995) has described the vegetation–atmosphere relationship as one of ''accommodation,'' whereby vegetation adjusts to atmospheric forcing (e.g., an increase or decrease in humidity) through stomatal control and extraction of soil moisture. Extended periods of drought, however, can result in feedbacks that may exacerbate stressed conditions. The absence of fair weather cumulus clouds can further aggravate extreme conditions, whereby increased environmental stress on vegetation [evidenced by a decrease in evapotranspiration (ET) or an increase in canopy resistance] leads to a drier atmosphere, further reducing ET (McNaughton and Jarvis 1991).

Therefore, the principal goals of this paper are to present an inter- and intraseasonal analysis of 1) the thermodynamic properties of the mixed layer, 2) BLcu frequency and occurrence, and 3) the light and energy environment just above a mixed deciduous forest canopy in the northeastern United States. We then link observations of turbulent fluxes of heat, moisture, and CO_2 with the presence of BLcu. This results in a more comprehensive description of the impact these clouds have on ET and net carbon uptake.

Section 2 will summarize the data used in this study and section 3 will present the climatology of land–atmosphere exchange and BLcu, empirical relationships between BLcu occurrence and mixed-layer characteristics, and empirical parameterizations resulting from sky type–insolation relationships. Also discussed in section 3 is the impact of the presence or absence of BLcu on carbon uptake and evapotranspiration. Section 4 will present the conclusions.

2. Data

a. ASOS

As part of the National Weather Service (NWS) Modernization Program, Automated Surface Observing System (ASOS) stations are being deployed throughout the United States. These stations measure, process, and disseminate surface observations including temperature, dewpoint, wind, pressure, precipitation, precipitation type, visibility, cloud ceiling, and sky conditions. Ultimately, over 900 ASOS stations will be deployed throughout the United States and its territories (NOAA 1998). The locations of all commissioned ASOS sites

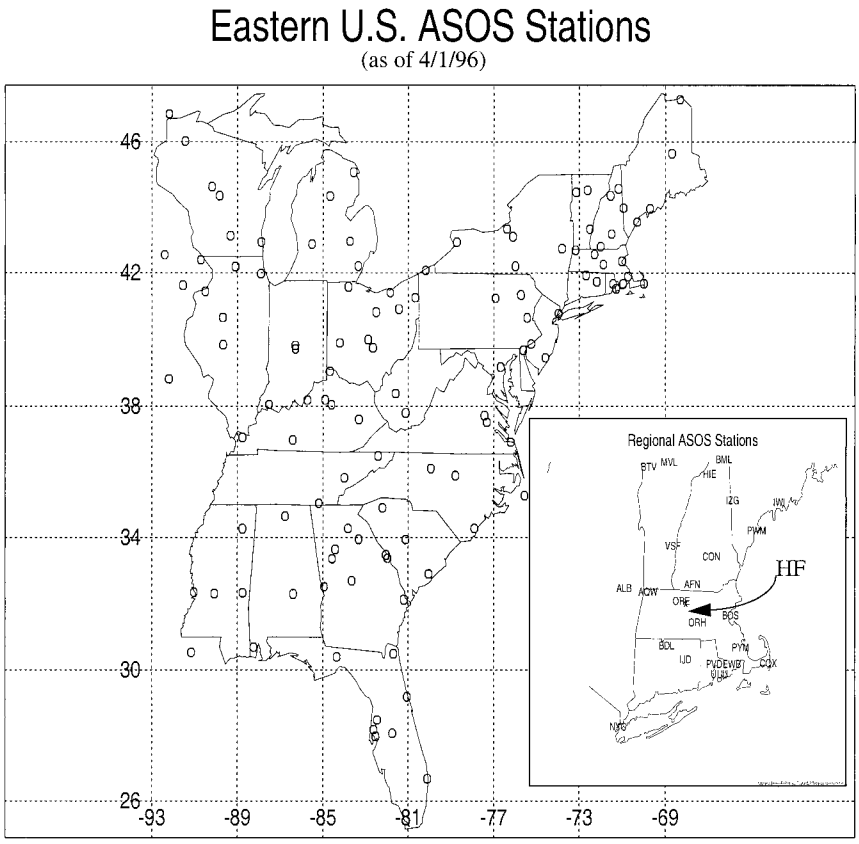

FIG. 1. Eastern U.S. commissioned ASOS stations, as of 1 Apr 1996. Inset: eastern NY and New England ASOS stations with HF site.

in the eastern United States as of April 1996 are shown in Fig. 1. Overall, the average interstation distance is about 170 km; in the northeastern United States, the average interstation distance is 100 km.

The cloud detector deployed at ASOS stations is a Vaisala 12CTK laser beam ceilometer, with a vertical measuring range of 12 000 ft (3658 m). It records ceiling heights every 30 s. The ASOS sky algorithm produces half-hourly averages of cloud heights and cloud cover every minute, double-weighting the last 10 min of observations to better handle rapidly changing sky conditions (NOAA 1998). For data prior to July 1996 [before the U.S. adoption of the international Aviation Routine Weather Report (METAR) surface observation code], the algorithm ''bins'' the sky conditions into clear (cloud cover $<$ 5%), scattered ($>$5% but $<$50%), broken ($>$50% but $<$87%), and overcast ($>$87%) conditions. For METAR reports, sky conditions include clear, few ($>$5% and $<$25%), scattered ($>$25% and $<$50%), broken ($>$50% and $<$88%), and overcast. Up to three levels of cloud layers are reported, with cloud heights rounded to the nearest 100 ft (30.5 m) below 5000 ft (1524 m), nearest 200 feet (61 m) above 5000 ft and below 10 000 ft (3048 m), and nearest 500 ft (152 m) above 10 000 ft (3030 m).

The large-scale ASOS boundary layer cloud analysis is derived from 5-min data archived by the National Climatic Data Center (NCDC). The high temporal resolution allows for the accurate depiction of cloud cover time fraction. The data consist of first-order commissioned ASOS sites from January 1995 through June 1996. Data from commissioned ASOS sites not available from NCDC, or subsequent to June 1996, have been supplemented by hourly and special observations archived at the University at Albany, State University of New York, Department of Earth and Atmospheric Sciences. Sounding data are from rawinsonde observations made twice daily (0000 and 1200 UTC) at Albany, New York, about 120 km to the west of Harvard Forest (HF), and obtained from the NCDC's Web site (www.noaa.ncdc.com) or the NWS Forecast Office in Albany (see Fig. 1 for location of sites referred to above). Long-term climate data are from the NCDC (1998).

b. Harvard Forest

Since 1991, groups from the Atmospheric Sciences Research Center (ASRC) and Harvard University have made nearly continuous atmospheric turbulence and trace gas measurements at the Environmental Monitoring Site (EMS) at HF, located in north-central Massa-

chusetts (42.54°N, 72.18°W). The forest is 50–70 yr old and contains a mixture of red oak, red maple, and hemlock. A variety of instruments record turbulent fluxes of CO_2, sensible heat and water vapor (by the eddy covariance method), solar and terrestrial radiation [including measurements from a multifilter rotating shadowband radiometer (MFRSR)], temperature, relative humidity and wind profiles, and trace gas (including CO_2) concentrations [see Wofsy et al. (1993), Munger et al. (1996), and Moore et al. (1996) for further details]. An ASOS station [Orange, Massachusetts (ORE)] is located less than 10 km to the west-northwest of the HF site. The nearest NCDC-archived station [Worcester, Massachusetts (ORH)] is about 39 km to the southeast.

3. Results and discussion

a. Surface and mixed-layer seasonal trends

In the northeastern United States, the spring season brings significant phenological and meteorological changes. Leaves emerge from deciduous trees and understory vegetation, and the basic state of the boundary layer is modified by increasing insolation and transpiring vegetation. This results in a decrease in the surface layer Bowen ratio ($B = H/\mathrm{LE}$), as shown by Moore et al. (1996), and a reduction in the seasonal surface daily diurnal temperature range (Schwartz 1996) and daily maximum temperature increase (Fitzjarrald et al. 2000). Earlier work by Moore et al. (1996) and Sakai et al. (1997) showed that, during spring, rapid changes in both solar and photosynthetically active radiation (PAR; 0.38–0.71 μm) albedos are correlated with increases in both the leaf area index (LAI) and the satellite-derived normalized difference vegetation index (NDVI). Figure 2 demonstrates the sequence of events, in terms of changes in the surface light, heat, and moisture environments, as leaves emerge at Harvard Forest. In Fig. 2a, which shows a 4-yr (1994–98) composite time series of LAI derived from PAR albedo measurements at Harvard Forest [following the Sakai et al. (1997) relations], leaf emergence occurs, on average, about day 140. This corresponds with the rapid drop in the surface layer Bowen ratio (Fig. 2b). Changes in seasonally averaged mixed-layer characteristics such as mixed-layer height (z_i) and specific humidity (q) are illustrated in Figs. 2c and 2d. Afternoon mixed-layer heights were visually estimated from the 0000 UTC (1900 or 2000 LT) profiles of potential temperature (θ) and q. The peak in z_i ($\sim$1350 m) at Albany (ALB) occurs near the time of maximum springtime sensible heat flux at HF (Fig. 2c, day 121), although the sensible heat flux remains high at HF two weeks after z_i begins to fall at ALB. This is likely due to the later onset of the growing season at HF, which is about 300 m higher than the ALB surface observation station. Subsequently, the mixed-layer specific humidity and surface latent heat flux increase significantly (Fig. 2d), both reaching a peak during the middle of the growing season. After this maximum, z_i averages around 1100 m. This is contrary to previous studies, which indicate larger differences between late winter and midsummer mean maximum mixing heights (e.g., Holzworth 1964, 1972). Holzworth (1972), in a 5-yr climatology of mixing heights, showed that z_i for ALB ranges from about 900 m during the winter months to a maximum of about 1800 m during the summer. Holzworth's estimates of mixing heights were made by determining the level at which the afternoon maximum surface temperature intersected the *morning* (1200 UTC) sounding. Thus, a completely adiabatic mixed layer was assumed, and advection and subsidence processes were ignored. This may explain the higher mixed-layer heights found during the summer (cf. with Fig. 2c). Because z_i was given for seasonal averages, the spring maximum is not apparent from the Holzworth (1972) analysis. The lower summertime mixed-layer heights and the springtime maximum in z_i found here may have important implications for air pollution modeling and analysis.

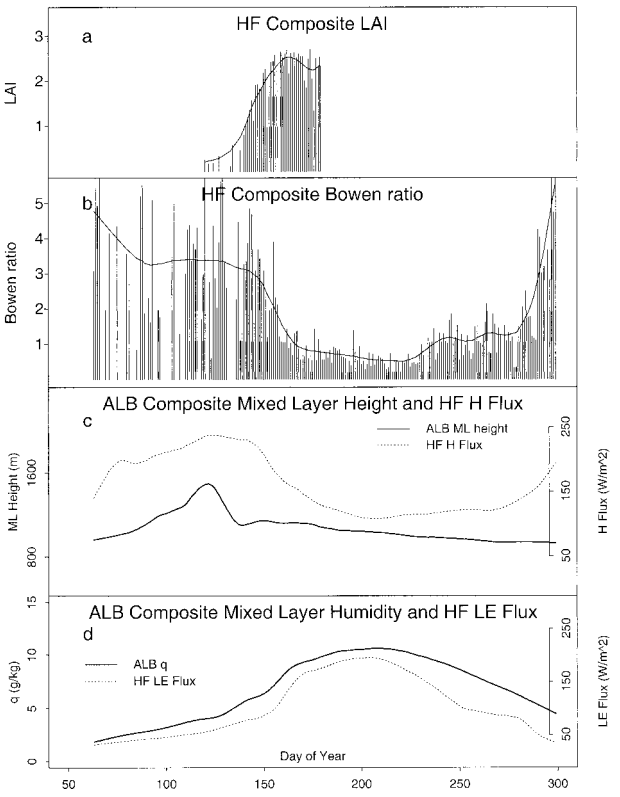

FIG. 2. (a) HF composite LAI for 1995–98 derived from midday (1000–1500 LT) solar albedo data using regression relationships from Sakai et al. (1997). Data are smoothed. (b) HF composite flux midday (1000–1500 LT) Bowen ratio for 1995–98. Solid line represents smoothed data. (c) Albany, NY, composite evening (0000 UTC or 1700 LT) mixed-layer height (solid line, in meters) and HF sensible heat flux (dashed line, in W m^{-2}). Data are smoothed. (d) Albany composite specific humidity (solid line, in g kg^{-1}) and HF latent heat flux (dashed line, in W m^{-2}) for 1995–98. Data are smoothed.

Fitzjarrald et al. (2001) demonstrate that rapid chang-

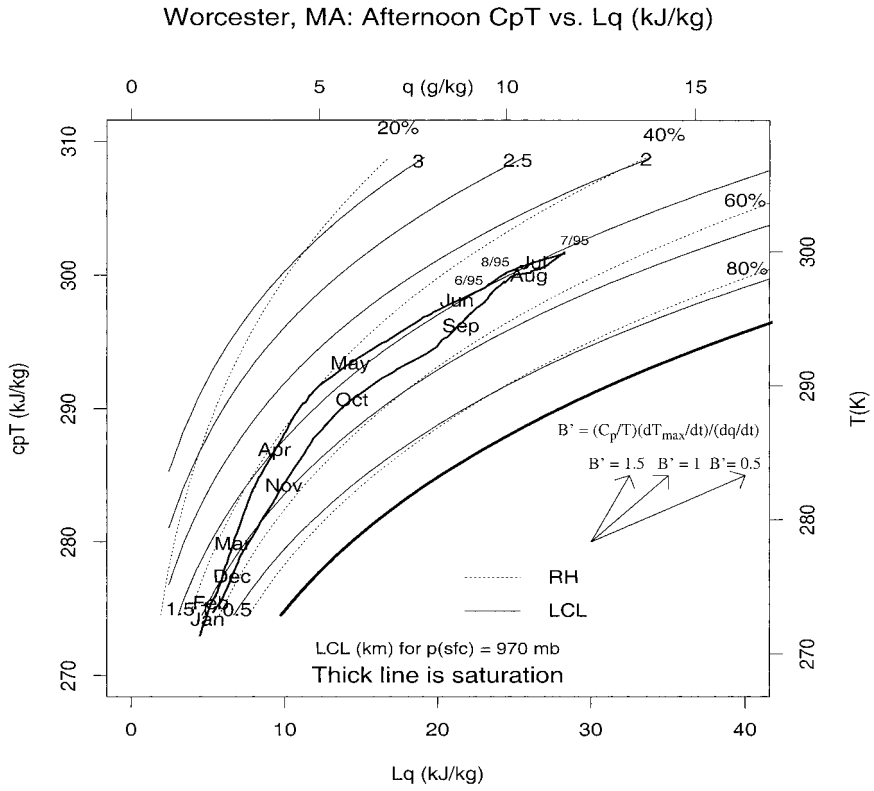

FIG. 3. Annual composite (1948–94) of afternoon maximum C_pT vs afternoon mean Lq (solid curve, in units of kJ kg^{-1}) for ORH. Temperature (right axis, in K) and specific humidity (top axis, in g kg^{-1}) are also shown. Thin solid curves sloping upward represent a surface-based lifting condensation level (based on an average surface pressure at ORH of 970 hPa), and thin dotted curves sloping upward to the right are relative humidity. Arrows in the right-hand corner are slope-based Bowen ratios. Dates represent conditions for Jun, Jul, and Aug 1995.

es in the heat and moisture fluxes instigated by the commencement of transpiration are detectable in long-term surface temperature and humidity time series composites. They present the budget equations for θ and q, integrated across a mixed layer of thickness (h) as

$$h\rho C_p \frac{\partial \theta_m}{\partial t} = H_s - [H_h - \mathrm{ADV}_{\theta m} - \mathrm{SRC}_\theta], \quad (1)$$

$$h\rho L \frac{\partial q_m}{\partial t} = \mathrm{LE}_0 - [\mathrm{LE}_h - \mathrm{ADV}_{qm} - \mathrm{SRC}_q], \quad (2)$$

where s and h refer to the surface and mixed-layer top, subscript m refers to a mixed-layer average, L is the latent heat of vaporization, C_p is the specific heat at constant pressure, and ADV_{xm} represents the mixed-layer average advective contribution ($x = \theta$ or q). The diabatic flux divergence term (SRC_θ, primarily radiative flux divergence) is important to the layer budget, though the mixed-layer moisture source (SRC_q) is probably negligible in long-term averages. Equations (1) and (2) can be combined to give a tendency Bowen ratio (Fitzjarrald et al. 2001):

$$B' \equiv \frac{\rho C_p}{\rho L} \frac{h\dfrac{\partial \theta_m}{\partial t}}{h\dfrac{\partial q_m}{\partial t}}. \quad (3)$$

Here, we take afternoon maximum temperature and mean humidity to represent mean mixed-layer conditions. Periods for which $B' \approx B$ occur if the bracketed terms in (1) are negligible or are proportional to the surface flux.

Seasonal changes in B', and their influence on cloudiness, can be illustrated on a conservative variable diagram (Fig. 3). The plot is similar to that introduced by Stommel (1947) and used by Paluch (1979) and Betts (1984, 1985) to study entrainment into clouds and boundary layer processes. A point on the diagram describes the thermodynamic state (q, θ) of the mixed layer, including its relative distance from saturation. Relatively small changes in mixed-layer heat and humidity can significantly alter the distance a parcel needs to rise in order to reach saturation and form clouds. As temperatures warm (after April), the lifting condensation level (LCL) is more sensitive to changes in $c_p\theta$ than

earlier in the winter (December–February), when moisture perturbations (Lq) are much more important (a function of the Clausius–Clapeyron equation). During the summer (June–August), however, changes in mixed-layer temperature or moisture have approximately equivalent effects on the LCL.

Throughout the winter season, cold temperatures and a fairly moist environment result in low LCLs (~1 km). During the winter–spring transition, the mixed layer warms rapidly, in response to intensifying daily insolation. This produces an annual maximum in LCL and sensible heat flux (cf. with Fig. 2c), and a corresponding minimum in afternoon relative humidity (RH). Shortly after leaf emergence (mid-May), however, in conjunction with the commencement of transpiration, B' falls abruptly from about 1.5 to 0.5, and remains constant until September, near the time of leaf senescence. This is consistent with measured Bowen ratio behavior at Harvard Forest and mixed-layer humidity (Fig. 2b) and z_i (Fig. 2c) trends at ALB. Furthermore, during the growing season, the boundary layer LCL (and RH) remain constant (around 1.5 km and 50%, respectively), reflecting the compensating effects of moistening with coincidental spring and summer heating (cf. with Figs. 2c,d).

The mixed-layer response to rapid changes in the inputs of heat and moisture is to seek a new equilibrium to balance the components of Eq. (3). During the spring transition, the daily tendencies of θ and q are approximately proportional to the surface fluxes in the northeastern United States: $C_p dT_{\max}/dt = \beta H$ and $Ldq/dt = \beta$LE, with $\beta \sim 0.05$ (Fitzjarrald et al. 2000). After leaf emergence, surface T and q change so as to maintain a constant LCL or RH throughout the summer. This equilibrium is maintained, in part, by the more frequent appearance of boundary layer cumulus clouds in the spring and summer months (see Figs. 5 and 6 and discussion below).

For this study, BLcu are defined as nonovercast conditions (<0.8 cloud cover) with a cloud base within 300 m of the surface-based LCL. The use of the LCL has been found to be a good surrogate for the daytime height of the convective boundary layer (Bunker et al. 1949; Fitzjarrald and Moore 1994). This criterion ensures that clouds classified as BLcu are necessarily coupled with the convective boundary layer. Figure 4 illustrates the link between the light environment at HF, in terms of insolation and its standard deviation, and BLcu and the surface-based LCL as observed at ORE. Note that large variations in insolation (or large values of its standard deviation, std$K\downarrow$) occur simultaneously with the presence of BLcu (values are based on a 20-min averaging period). Higher clouds, however, result in much less variation in insolation (or smaller std$K\downarrow$). Further analysis of these relationships will be given in section 3c.

Although the highest Bowen ratios, sensible heat fluxes, and mixed-layer heights occur before leaf-out, the appearance of BLcu, at least in the forested areas of central New England, is dependent upon the additional infusion of moisture from transpiring vegetation, as well as a decrease in $dT_{\max}/dt$ (see Figs. 2 and 3). Further discussion of BLcu climatology and its link with the forest–atmosphere exchange is given below.

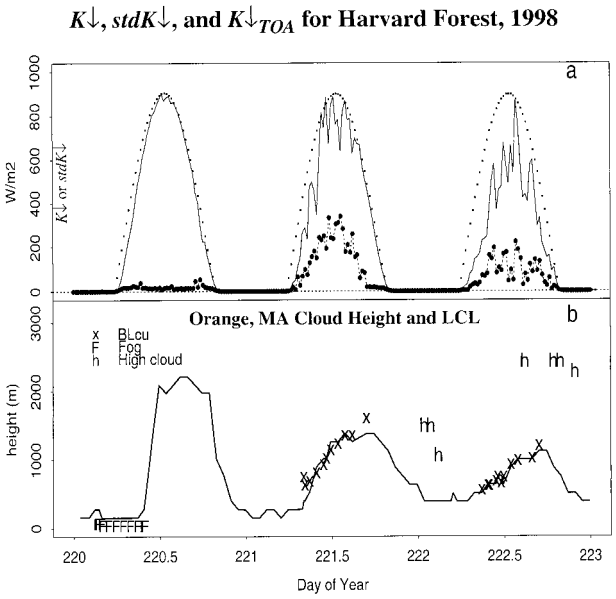

FIG. 4. (a) $K\downarrow$ (solid line), std$K\downarrow$ (dotted-dashed line), and 80% of TOA$K\downarrow$ (dotted line) (all in W m^{-2}) for HF, days 220–223, 1998. (b) ORE cloud height (h is high clouds, × is BLcu, and F is fog) and surface-based lifting condensation level (solid line) for days 220–223, 1998.

b. BLcu

Present surface-based cloud climatologies do not include specific occurrences of BLcu; such clouds fall within the World Meteorological Organization's (1969) (WMO) ''low'' cloud genus, cumulus. Stull (1992) defined his cloud analysis in terms of ''cover hours'' (the cloud cover fraction multiplied by the number of hours clouds are observed). He subdivided his cloud groups based on the reported WMO cloud type and included a boundary layer clouds subset (cumulus, cumulus fractus, towering cumulus, and stratocumulus). Using one year of data from a single NWS station (Madison, Wisconsin), he found that fair weather cumulus clouds accounted for 33% of all cloud reports, with a maximum frequency (upward of 50%) during the summer months. Warren et al. (1986), produced a comprehensive land-based cloud climatology based on 10 yr (1971–81) of surface observations from 3-hourly synoptic reports averaged onto 5° × 5° grids. They subdivided their analysis into several different cloud groups, finding that cumulus frequency in the eastern United States generally peaks during summer months (June–August) and ranges from 17% over coastal New England to 32% over the mid-Atlantic states. The local time of maximum cu-

mulus cloud amount (phase of the diurnal cycle) varies from 1300 LT over the southeast and Midwest to 1400 LT over the northeastern United States.

Surface-based climatologies suffer from human observational constraints such as the ''packing effect'' (see NOAA 1998; Bradley and Lewis 1998); observers tend to overestimate the cloud coverage because clouds near the horizon appear to blend together or overlap. Satellite climatologies, such as the International Satellite Cloud Climatology Project (ISCCP) dataset (Rossow and Schiffer 1991), where cloud type is inferred from measurements of visible and infrared satellite imagery, are constrained by coarse resolution (Wielicki and Welch 1986) and are limited in estimating low-cloud type and coverage by other measurement constraints, such as small temperature differences between the land surface and BLcu cloud top (Benner and Curry 1998), and obscuring higher cloud decks. Wielicki and Welch (1986), showed that at 1-km resolution there are considerable differences in both observed range of cloud reflectance and the sensitivity of derived cloud fraction to variations in cloud threshold variance. They found that increasing the spatial resolution to about one-fifth of the area-averaged cloud diameter would be sufficient to accurately depict spatial characteristics of a fair weather cumulus cloud field. For a typical cumulus cloud of 1 km, that would require a resolution of 200 m for accurate cloud fraction estimates, well below the 1-km visible resolution currently available on Geostationary Operational Environmental Satellites (GOES) (but within the resolution of *SPOT* and *LANDSAT*; however, satellite imagery from these sources for a specific geographic area is limited temporally).

In a comparison between surface-based and the ISCCP cloud climatologies, Rossow et al. (1993) found differences as great as 25% for small cumulus clouds. Ultimately, by using ASOS cloud cover and cloud ceiling data, a more objective surface-based cloud climatology, based on uniform instrumentation and data acquisition algorithms, will be possible. ASOS, however, is not without its limitations, notably its inability to detect clouds above either 12 000 ft or an obscuring ceiling.

The frequency of particular daytime sky conditions at ORE is shown in Fig. 5. Note that ''clear'' skies may include occurrences of high clouds (those above 12 000 ft that are not detectable by the ASOS ceilometer). For the years considered (1995–98), there is a growing season maximum in the occurrence of BLcu, in general agreement with Stull's 1990 observations of boundary layer clouds at Madison (Stull 1992). There is a corresponding minimum in low, overcast conditions during the spring–summer period, whereas, except in 1995, ASOS clear sky conditions are rather uniform throughout the year. The growing season maximum in BLcu is most apparent during 1997 and 1998.

A monthly BLcu histogram of BLcu days (Fig. 6) shows a distinct summer season peak in BLcu days. Here, a BLcu day is defined as one where the BLcu

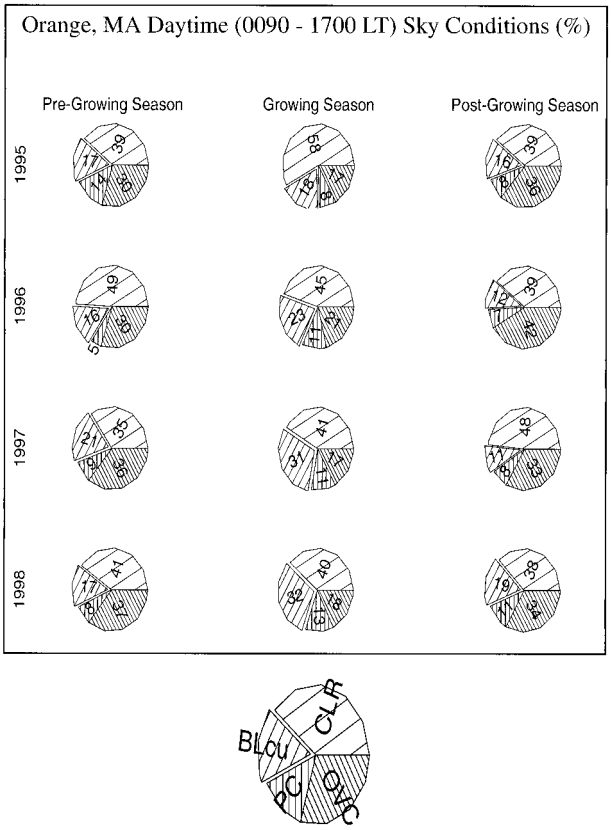

FIG. 5. Frequency diagram for 4 yrs of daytime (0900–1700 LT) hourly sky conditions from ORE, with each year divided into thirds representing pre-leaf-out, growing season, and fall senescence. Sky conditions are subdivided into four categories: clear (<2/10); BLcu (>2/10 and <8/10, and ceiling height within 300 m of surface-based LCL); non-BLcu (>2/10 and <8/10, but not within BLcu-LCL constraint); and overcast (>8/10).

conditions given above are met for at least two consecutive hours. As in Fig. 5, the summer of 1995 (especially June and August) featured relatively few BLcu as compared with subsequent years. The weather for both months was warm and dry (see Tables 1, 2, and 3). Based on surface data from ORH, both June and August feature LCLs of 250 and 430 m above the long-term mean (see Fig. 3 and Table 3). Although July was also a warm month, moister conditions compensated for the above-normal temperatures. Consequently, the July LCL was not significantly different from the mean, and the number of BLcu days was not unusually small.

To examine seasonal trends over the eastern United States, monthly BLcu time frequency (BLcu time fraction divided by the total cloud time fraction) was examined at all eastern U.S. ASOS stations for January–June 1996 (Fig. 7). During the winter and early spring (January–March), BLcu cloud fraction is generally below 30%. By April, cloud fraction has increased significantly over the southeast and mid-Atlantic states, with a distinct maximum over Florida (indicative of sea-breeze convergence

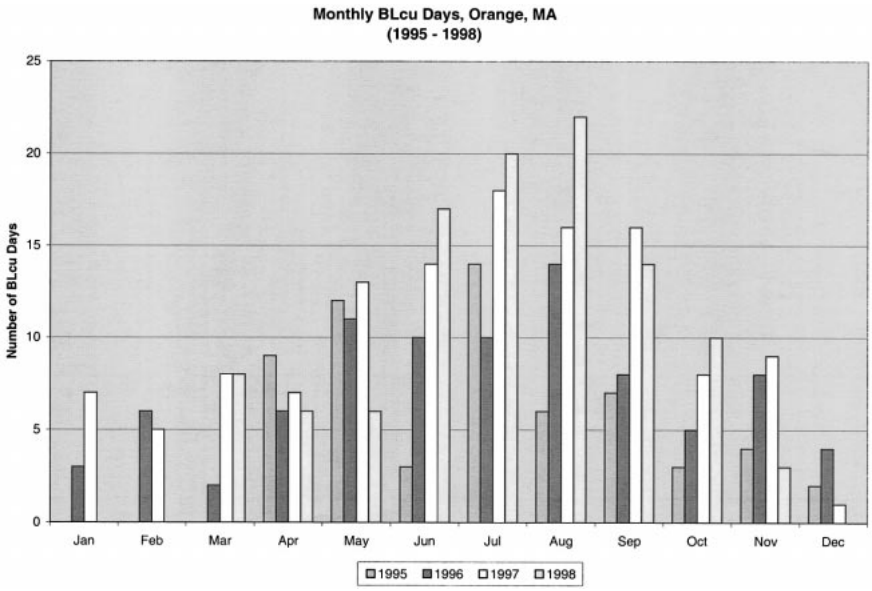

FIG. 6. Monthly BLcu days at Orange, MA, for 1995–98. A BLcu day is defined as BLcu conditions occurring for at least two consecutive hours during 0900–1700 LT.

common during the spring–summer season). From May to June however, the daytime skies over a very large area of the mid-Atlantic states are dominated by BLcu (>70%). Both the seasonal trend and location of maxima are in general agreement with the land surface cumulus climatology of Warren et al. (1986), which shows the summer season maximum in frequency in the southeast and inland mid-Atlantic states. The ISCCP 11-yr daytime cumulus cloud climatology also shows overall agreement in the seasonal trend in frequency, although occurrences are up to 25% lower (Rossow et al. 1993). The seasonal *amplitude* of BLcu time frequency ranges from three-tenths in northern New England to nearly seven-tenths in the mid-Atlantic states. Moreover, the month-to-month maxima in the *rate of increase* is later as one moves from south to north. It varies in time from February in the southeastern states to June in the mid-Atlantic and northeast. This compares favorably with other indices of spring, such as the NDVI and changes in B' (Fitzjarrald et al. 2001).

Because BLcu are a daytime phenomenon, influenced by land surface characteristics such as topography and land-cover type, the ASOS dataset was examined for growing season diurnal variability. Local and regional variations in BLcu onset and coverage are illustrated in Fig. 8, a series of visible satellite images showing a typical diurnal sequence of BLcu evolution over the northeastern United States. BLcu first appear over the mountainous terrain of the Catskills and Adirondacks of New York, and the Green and White Mountains of Vermont and New Hampshire (Figs. 8a–c). By 1215 LT (Fig. 8c), the Hudson, Mohawk, and Connecticut River valleys are clearly discernible. Also, clouds demarcating a sea-breeze convergence zone near the southern New England coast appear. This feature moves inland as the afternoon progresses (Figs. 8d,e). Finally, during mid-afternoon (Figs. 8e,f), the valleys fill with BLcu as clouds are advected from the more mountainous terrain, and locally generated thermals are able to reach their respective LCLs.

The station location bias of cloud onset and peak coverage time illustrated by the above example is apparent from Fig. 9, a plot of the diurnal sequence of BLcu time fraction for a subset of the ASOS stations. Three distinct regimes were identified; mountain or plateau, valley, and coastal. Onset times were subjectively set at cloud fractions exceeding 5%. Station locations were determined by examining topographic maps. At

TABLE 1. Tully Lake average monthly maximum temperature (°C) (1961–90).

Year	Jan	Feb	Mar	Apr	May	Jun	Jul	Aug	Sep	Oct	Nov	Dec	Annual
1995	1.5	−0.1	9.9	13.2	19.5	27.2	29.8	29.1	22.7	19.2	6.9	−1.6	14.8
1996	1.0	2.4	8.0	13.7	20.4	26.3	27.4	28.8	22.6	16.4	7.5	3.3	14.8
1997	1.2	4.4	5.5	12.7	19.2	27.5	28.8	27.0	22.4	15.2	7.0	3.2	14.5
1998	NA	NA	7.4	16.4	22.3	24.0	28.7	28.2	24.3	NA	NA	NA	NA
Normal	−1.2	0.3	6.2	13.2	20.2	25.0	27.8	26.5	21.7	14.8	8.3	1.0	13.7

TABLE 2. Tully Lake average monthly precipitation (mm) (1961–90).

Year	Jan	Feb	Mar	Apr	May	Jun	Jul	Aug	Sep	Oct	Nov	Dec	Annual
1995	97	68	67	64	81	70	84	47	66	258	110	69	1081
1996	167	69	66	187	118	114	197	7	160	109	119	197	1510
1997	77	55	93	125	87	14	110	135	24	61	137	66	984
1998	141	65	106	54	63	231	94	24	62	116	59	NA	NA
Normal	82	77	85	91	98	95	100	104	82	86	100	94	1094

mountain or plateau stations, BLcu first appear around 0900 LT and reach a coverage peak shortly after 1300 LT. This is likely due to differential heating producing a mountain–valley circulation with upslope flow (anabatic winds), during the day. Coastal stations have a similar onset time, with a maximum coverage at 1300 LT, a consequence of sea-breeze convergence zones that set up along the coast and subsequently move inland (see Fig. 8 and discussion above). Finally, for inland valley locales, BLcu onset is complicated by the decay of morning stratocumulus breakup, which occurs between 0800 and 1000 LT. There is a midafternoon peak near 1500 LT. The same mountain–valley breeze circulation that produces the early onset and peak times over mountain stations induces divergent flow over the valleys, with a suppression of cloudiness (lower cloud fractions). For peak coverage time the station location bias is about 2 h between mountain and valley locales. Gibson and Von der Haar (1990) found similar topographic impacts on cloud onset and frequency in a satellite study of the southeastern United States.

c. Sky cover and the light environment

The presence of BLcu alters the character of the light environment within and above the forest canopy. These clouds produce ground shading, which moderates surface temperatures, and provide an additional source of diffuse radiation, which penetrates deeper into the forest canopy than does solar beam radiation (Jarvis et al. 1985). Studies have shown enhanced forest CO_2 uptake on days featuring clouds (Price and Black 1990; Hollinger et al. 1994; Fitzjarrald et al. 1995; Fan et al. 1995; Goulden et al. 1997; Baldocchi 1997).

TABLE 3. Monthly maximum temperature (°C), mean specific humidity (g kg^{-1}), and surface-based LCL (m) for Worcester, MA.

		Jun	Jul	Aug
1995	T (°C)	24.9	27.9	26.3
	q (g kg^{-1})	8.8	11.6	9.5
	LCL (m)	1676	1509	1679
1996	T (°C)	23.3	25.6	24.8
	q (g kg^{-1})	10.3	11.6	11.8
	LCL (m)	1157	1228	1089
1997	T (°C)	23.9	25.7	24.1
	q (g kg^{-1})	8.3	9.8	10.3
	LCL (m)	1621	1542	1256
1998	T (°C)	21.2	25.9	26.0
	q (g kg^{-1})	9.9	11.5	11.8
	LCL (m)	973	1273	1237
Mean*	T (°C)	23.7	25.3	25.1
	q (g kg^{-1})	8.8	9.5	10.6
	LCL (m)	1492	1549	1326

* Mean is based on a 44-yr period of record.

Relationships between the light environment and cloud cover go back to the early work of Kimball (1919, 1928), Angstrom (1924), and Prescott (1940). The equations have the general form

$$K\downarrow/K\downarrow_{\mathrm{TOA}} = a + bC, \tag{4}$$

where $K\downarrow$ is the downward shortwave radiation, $K\downarrow_{\mathrm{TOA}}$ is the maximum, top-of-the-atmosphere (TOA) downward shortwave radiation, C is the measured or observed cloud cover (in tenths), and a and b are regression coefficients. Later work by Pochop et al. (1968) and Brutsaert and Sugita (1992) also uses this form (see Table 4 for a summary of radiation–cloud cover relationships). For this study, we compared hourly cloud cover reports from the ASOS station at ORE with hourly averaged radiation data from HF, but we take $K\downarrow_{\mathrm{TOA}}$ to be about 80% of the TOA maximum. The choice of this theoretical maximum better approximates the maximum clear sky $K\downarrow$ observed at HF, which is about 1070 W m^{-2}, as compared with the TOA maximum of about 1290 W m^{-2}, for HF's location. Although ORE is about 10 km from the HF EMS site, given an average cloud drift of 10 m s^{-1}, the cloud cover algorithm (discussed above), on typical days, should represent a spatially averaged observed sky condition for a radius of 10 km. Therefore, on most days, sky conditions at both ORE and HF should be similar (see Fig. 4).

Falconer (1948, 1965) suggested that cloud type could be determined by reference to a time series of downward shortwave radiation. Fitzjarrald (1995) identified the signature of BLcu at HF by examining the time series of the standard deviation of downward shortwave radiation (std$K\downarrow$) and cloud base. Recall the comparison of cloud cover at ORE with radiation data from HF (Fig. 4). Day 220 is a clear day, with $K\downarrow$ almost approaching $K\downarrow_{\mathrm{TOA}}$ (Fig. 4a), and no clouds reported at ORE (Fig. 4b). On day 221, however, BLcu appear during midmorning and are present until late afternoon. This is manifested in the simultaneous appearance of large values of std$K\downarrow$. Moreover, $K\downarrow$ occasionally exceeds $K\downarrow_{\mathrm{TOA}}$ indicating downward reflection from the sides of BLcu. Finally, on day 222, BLcu again form during the morning (simultaneously with high values of

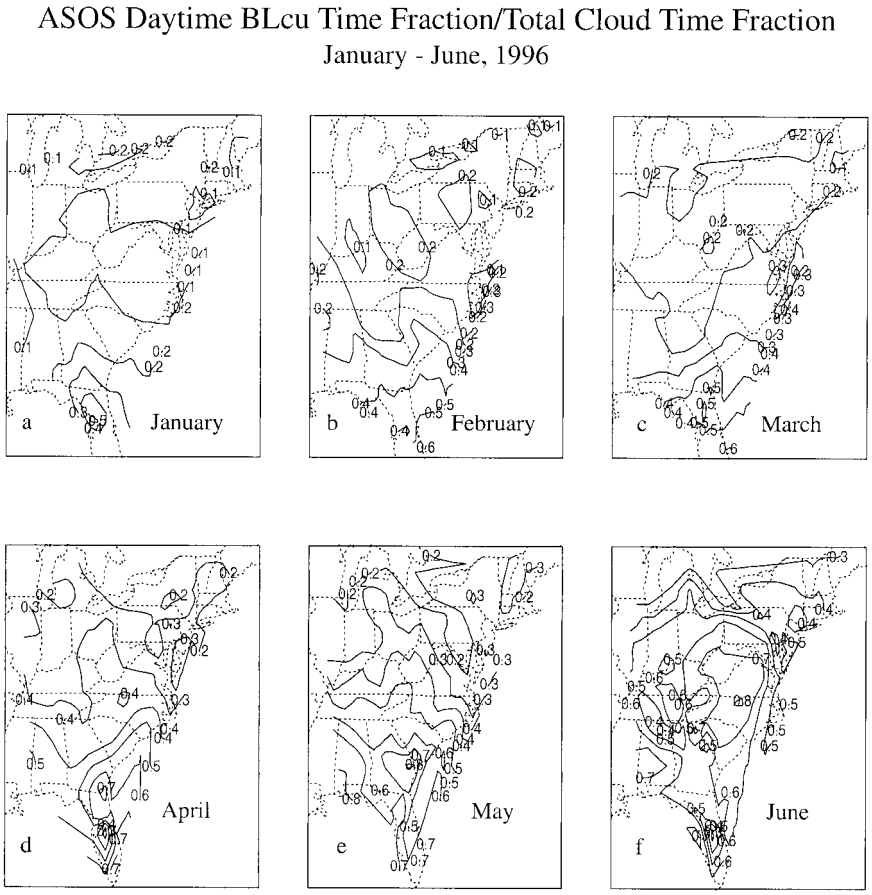

FIG. 7. Monthly daytime boundary layer cumulus cloud time fraction (number of occurrences of boundary layer cumulus divided by the number of occurrences of all clouds) for Jan–Jun [(a)–(f)] 1996 over the eastern United States. Contours are in tenths.

std$K\downarrow$), but during the early afternoon high clouds appear, with a concomitant drop in std$K\downarrow$. The coupled appearance of BLcu with large variations in std$K\downarrow$ confirms that sky conditions as recorded at ORE are also representative of conditions at HF.

A plot of normalized $K\downarrow$ (observed $K\downarrow/K\downarrow_{\text{TOA}}$) versus cloud cover (Fig. 10a) shows that clear and overcast days are tightly grouped in the upper left (low cloud cover, high $K\downarrow$) and lower right (high cloud cover, low $K\downarrow$), with BLcu and other partly cloudy conditions spread through the middle. As the ASOS ceilometer did not measure cloud heights above 12 000 ft, it is likely that some ''clear'' days featured some high or even some middle cloud decks (within the cirrus and alto cloud genera). Nevertheless, the overall fit is very good.

Figure 10b shows that a cloud cover of about 0.5 generates the largest values of std$K\downarrow$. Most of the larger values of normalized std$K\downarrow$ are BLcu days; note also how clear and overcast days are confined mostly to low values of std$K\downarrow$. Overall, a quadratic fit to the data is reasonably good ($r^2 = 0.48$) and is significant at the 99% confidence level, indicative of good correspondence between high std$K\downarrow$ days and BLcu events. Curves for 1996–98 yielded similar results. Finally, a polynomial regression of std$K\downarrow$, $K\downarrow$, and cloud fraction (Fig. 11) shows a very good ($r^2 \sim 0.78$) quantitative relationship among the variables. The regression is given by

$$C = 114.6 - 0.33K\downarrow + 0.48\text{std}K\downarrow + 0.00022K\downarrow^2 - 0.00014\text{std}K\downarrow^2 - 0.0004\text{std}K\downarrow K\downarrow, \quad (5)$$

where C represents the cloud cover (%), and $K\downarrow$ and std$K\downarrow$ are in W m^{-2}. At the extremes, low $K\downarrow$ and low std$K\downarrow$ days are associated with overcast conditions, whereas high $K\downarrow$ and low std$K\downarrow$ days feature generally clear skies. For cloud coverage approaching 50%, an absolute maximum in std$K\downarrow$ is associated with a relative maxima in $K\downarrow$; the figure thus combines the parameterizations realized separately in Fig 10.

We have derived a diffuse fraction relationship for Harvard Forest. They are given by

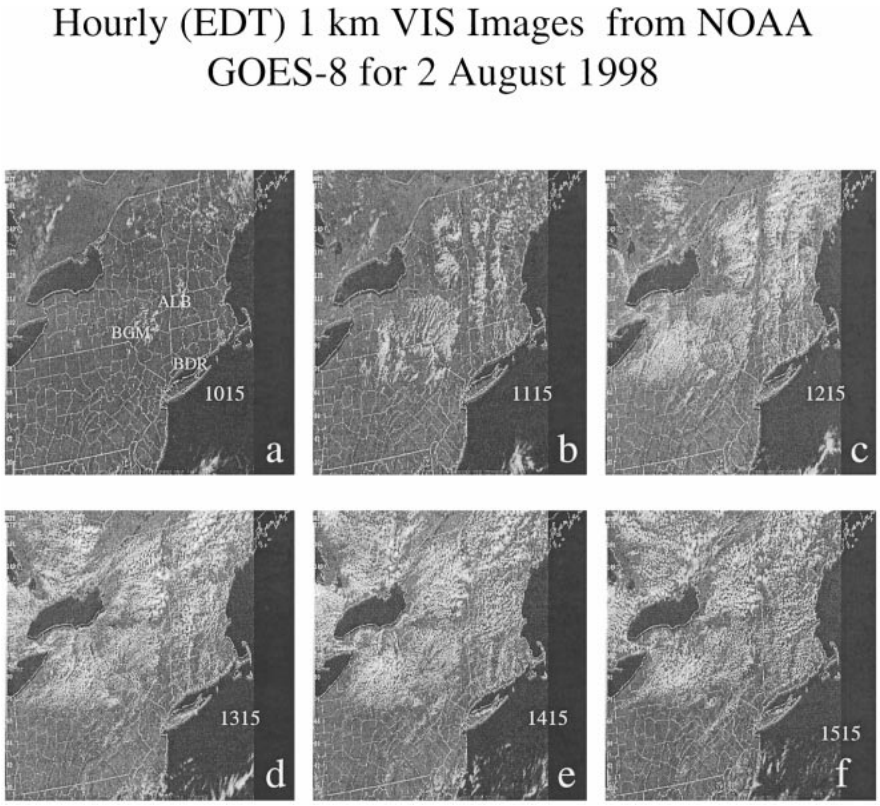

FIG. 8. Hourly (1015–1515 EDT) 1-km visible images from NOAA *GOES-8* satellite for 2 Aug 1998. Locations for ALB, Binghamton, NY(BGM), and Bridgeport, CT (BDR), are indicated in (a).

$$\frac{K_{\text{diff}}}{K\downarrow} = 1.0 \qquad \text{for } K\downarrow/K\downarrow_{\text{TOA}} < 0.3, \quad (6)$$

and

$$\frac{K_{\text{diff}}}{K\downarrow} = 0.84 + 1.77\left(\frac{K\downarrow}{K\downarrow_{\text{TOA}}}\right) - 4.89\left(\frac{K\downarrow}{K\downarrow_{\text{TOA}}}\right)^2 + 2.07\left(\frac{K\downarrow}{K\downarrow_{\text{TOA}}}\right)^3 \quad \text{for } K\downarrow/K\downarrow_{\text{TOA}} > 0.3, \quad (7)$$

where K_{diff} represents the absolute diffuse radiation obtained from the MFRSR. The cloud cover and diffuse fraction relationship are shown in Fig. 12. The overall fit is very good (explaining 79% of the variation), with $K_{\text{diff}}/K\downarrow$ approaching 1 as skies become overcast. Monteith and Unsworth (1990) indicate that the absolute level of K_{diff} reaches a maximum at cloud fractions of about 0.5, but they offer no evidence for this conclusion. For HF and ORE, there is a peak in K_{diff} at about 0.6 cloud cover fraction (not shown), but the correlation is very weak ($r^2 \sim 0.16$). The impact of variable cloud cover on forest–atmosphere exchange is discussed below.

d. Sky cover and vegetation response

To examine the impact BLcu have on vegetation–atmosphere exchange, various parameters were binned according to the sky categories specified above (clear, BLcu, non-BLcu clouds, overcast) for afternoons (1200–1600 LT) at HF during days 159–259, 1995–98 (Table 5). The standard errors for the variables are also given. During 1995, F_{CO_2} (uptake) was much higher (52%) on BLcu days as compared with the clear regime; a Student's t-test shows that the difference in these means is significant at the 95% level. Note that F_{CO_2} represents a net exchange of CO_2 above the forest; it includes both respiratory and photosynthetic fluxes. For 1996–98, net carbon uptake is still enhanced (31%, 14%, and 27%, respectively) on BLcu days. These findings are in general agreement with other studies that show higher radiation use efficiency on ''cloudy'' days for both temperate deciduous (Baldocchi 1997), broadleafed evergreen forests (Hollinger et al. 1994) and boreal forests (Fan et al. 1995; Goulden et al. 1997). For those studies, however, cloud type was not specifically analyzed; sky type (either clear or cloudy) was classified according to diffuse fraction, using values greater than 0.5 or 0.7. These correspond to cloud fractions of 0.5

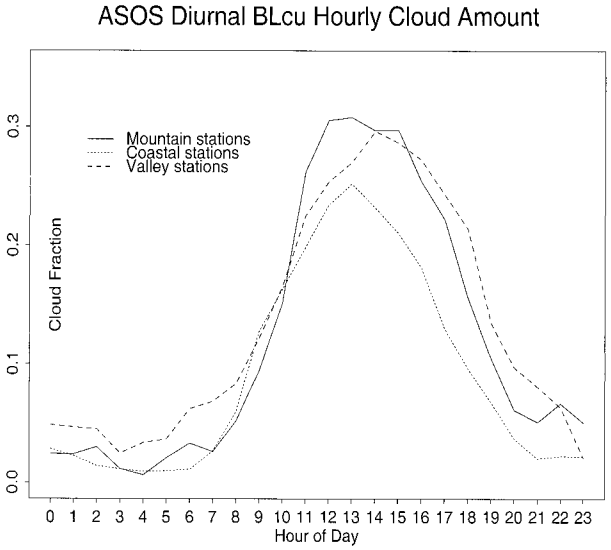

FIG. 9. ASOS diurnal boundary layer cumulus time-averaged cloud amount (frequency of occurrence × amount of cloud when present), days 120–160, 1996 for mountain (solid line), coastal (dotted line), and valley (dashed line) stations.

or above (see Fig. 12). [Goulden et al. (1996) state that ''prolonged periods of cloudiness'' reduced net carbon uptake during several summer periods at HF; we take this to mean during overcast conditions, not during BLcu days.]

A possible explanation for the large disparity in net carbon uptake and sky regime during 1995 lies in the rather extreme drought conditions that occurred throughout the 1995 growing season. The excessive warmth and lack of precipitation are apparent from Tables 1 and 2, which present temperature and precipitation data from Tully Lake, an NWS Cooperative Observing Station a few kilometers north of HF. For 1995, spring and summer precipitation were well below climatological normals, with a 6-month deficit of 176 mm. This is reflected in the very low volumetric soil moisture recorded at the HF EMS site during 1995 (Savage et al. 1998), which for the top 10 cm remained below 0.1 cm^3 cm^{-3} for much of the growing season (as compared with >0.2 cm^3 cm^{-3} during all of the 1996–98 growing seasons), reaching its nadir in late August. Furthermore, only 1995 featured a large difference in vapor pressure deficit (VPD) between the two sky regimes (~9 hPa). Thus, a season-long drought, high temperatures, reduced soil moisture, and high VPDs likely contributed to the larger reductions in afternoon C uptake observed on clear days during 1995. However, the presence of BLcu seems to have ameliorated the excessive environmental stresses (high temperatures and VPDs) associated with long-term drought conditions.

Baldocchi (1997) has suggested that both physical and physiological processes may be responsible for the enhanced F_{CO_2} observed on partly cloudy days. On clear days, leaves at the top of the canopy become light saturated and warmer than leaves in the shadier lower canopy. Consequently, these leaves experience enhanced respiration, which lowers rates of net photosynthesis (Baldocchi and Harley 1995). Goulden et al. (1996), however, have shown that there was a significant *decrease* in soil respiration (a consequence of reduced soil moisture) that more than offset the simultaneous decrease in photosynthesis observed at HF during 1995. It may be that the enhancement of F_{CO_2} observed at HF during BLcu days during 1995 was at least partially due to the significant reduction in respiration (30% lower as compared with other years), which was probably particularly acute on hot, cloudless days. Under the water-stressed conditions that existed during 1995, both the understory and canopy contribution (as well as other nonvegetation sources of evaporation) to ET was reduced. This may explain why ET for both clear and BLcu regimes is less (~5 mm day^{-1}) than subsequent years (Table 5). During 1996–98, when water availability was not a limiting factor, ET was greater (by 1–3 mm day^{-1}) during clear days, as compared with BLcu

TABLE 4. Radiation–sky cover relationships.

Authors	Relationship
Kimball (1928)[a]	$K\downarrow/K\downarrow_{\text{TOA}} = 0.29 + 0.71(1.0 - C)$
Pochop et al. (1968)	$K\downarrow/K\downarrow_{\text{TOA}} = 0.762 - 0.385C$
Burridge and Gadd (1974)[b]	$K\downarrow/K\downarrow_{\text{TOA}} = (1 - 0.4c_L)(1 - 0.7c_M)(1 - 0.4c_H)$
Brutsaert and Sugita (1992)	$K\downarrow/K\downarrow_{\text{TOA}} = 0.8060 - 0.4261C$
Hurley and Boers (1996)[c]	1. $K\downarrow/K\downarrow_{\text{TOA}} = (1 - 0.09C_L)(1 - 0.14C_M)(1 - 0.05C_H)$
	2. $K\downarrow/K\downarrow_{\text{TOA}} = (1 - 0.33C_L)(1 - 0.54C_M)(1 - 0.39C_H)$
This study	$K\downarrow/K\downarrow_{\text{TOA}} = 0.91 - 0.7C$
This study	$\text{std}K\downarrow/K\downarrow_{\text{TOA}} = 0.05 + 0.49C - 0.52C^2$
This study	$C(\%) = 114.6 - 0.33K\downarrow + 0.48\text{std}K\downarrow + 0.00022K\downarrow^2 - 0.00014\text{std}K\downarrow^2 - 0.0004\text{std}K\downarrow K\downarrow$

[a] C represents sky fraction.
[b] C_L represents low clouds; C_M is middle clouds; and C_H is high clouds (Stull 1988).
[c] The first relationship is for cumulus/cirrus clouds; the second is for stratus clouds.

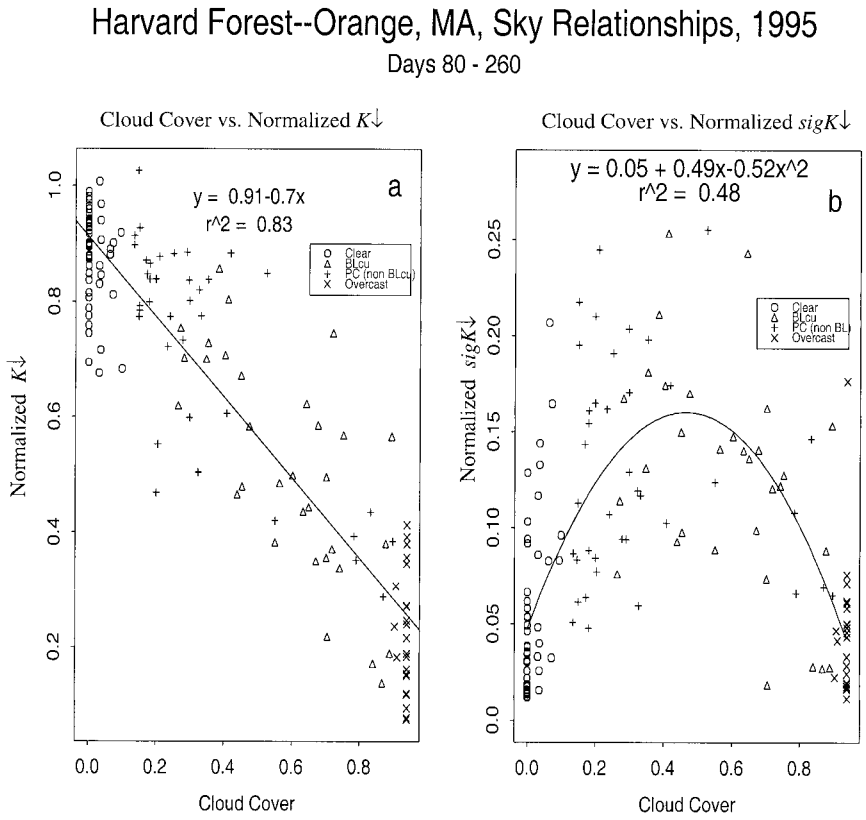

FIG. 10. (a) Total cloud cover as measured at ORE vs normalized $K\downarrow$ from HF for days 80–260, 1995. Symbols represent clear days (circles), BLcu days (triangles), non-BLcu but not overcast days (pluses), and overcast days (crosses). The solid line is a least squares fit to the data. (b) As in (a), but total cloud cover fraction vs normalized std$K\downarrow$. The curved line is a quadratic fit to the data.

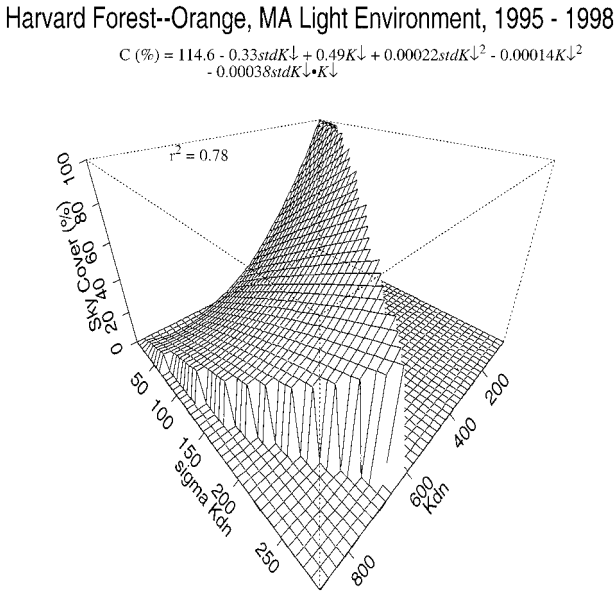

FIG. 11. Total cloud cover (%) (at ORE) vs $K\downarrow$ and std$K\downarrow$ (W m^{-2}) (at HF) for days 80–260 during 1995–98. The surface represents a polynomial fit to the data.

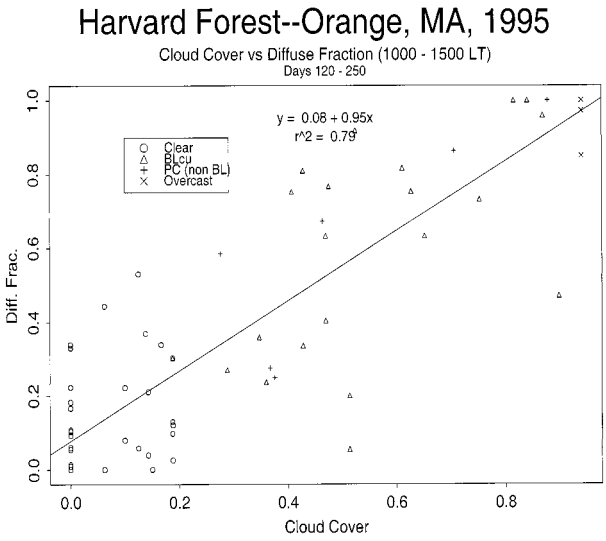

FIG. 12. Midday (1000–1500 LT) cloud cover fraction vs diffuse radiation fraction for HF and ORE, days 150–250, 1995.

TABLE 5. Harvard Forest environmental variables (with standard errors) for afternoon (1200–1600 LT) sky regimes (days 160–260).

Regime	Variable	1995		1996		1997		1998	
CLR	Days	20		15		12		8	
BLcu		24		44		60		60	
OVC		7		11		8		6	
CLR	$F\text{co}_2$ (mg m^{-2} s^{-1})	−0.31	0.07	−0.42	0.15	−0.43	0.06	−0.36	0.09
BL		−0.47	0.08	−0.55	0.08	−0.5	0.03	−0.46	0.05
OVC		−0.13	0.11	−0.15	0.11	−0.17	0.07	−0.25	0.16
CLR	ET (mm day^{-1})	5.79	1.45	11.08	1.52	9.65	1.03	7.26	1.95
BL		5.85	1.00	8.03	1.25	8.16	0.65	6.25	0.72
OVC		0.67	0.64	0.52	0.07	1.27	0.78	5.81	3.00
CLR	VPD (hPa)	23.3	2.98	15.05	2.01	16.93	2.63	15.38	3.69
BL		14.88	2.09	15.88	1.69	15.2	1.83	16.56	1.24
OVC		7.01	6.40	2.26	2.04	15.17	4.38	2.25	2.05
CLR	WUE (mg g^{-1})	4.84	2.86	5.59	2.08	5.5	0.85	5.75	4.04
BL		7.22	2.35	8.11	1.84	5.65	0.73	6.11	2.15
OVC		7.3	4.69	10.1	4.36	7.97	5.05	7.87	4.74
CLR	$K\downarrow$ (W m^{-2})	747	22	642	41	830	29	725	32
BL		620	38	600	44	630	26	625	24
OVC		130	34	156	25	153	27	139	27
CLR	$\sigma K\downarrow$ (W m^{-2})	17	9	41	13	13	9	44	13
BL		130	14	97	14	138	10	155	11
OVC		23	5	25	9	25	6	23	7

days. With no clouds present, net radiation is greater and ET is higher.

For 1996–98, afternoon F_{CO_2} enhancement is smaller, as compared with 1995. This may be a result of more seasonable weather conditions, with temperature and precipitation near climatological normals (see Tables 1 and 2). Soil moisture values were higher than in 1995 (above 0.2 cm^3 cm^{-3}). Individual months (August 1996, June 1997, and August 1998) did feature significant dry periods, but no single weather regime dominated the growing season, as in 1995.

Given the reduced F_{CO_2} on clear days observed during 1995–98, water use efficiency (WUE), given here by the CO$_2$–water vapor flux ratio (F_{CO_2}/ET), is higher on BLcu days (7.22 and 8.11 mg g^{-1}), as compared with clear days (4.84 and 5.59 mg g^{-1}) in both 1995 and 1996, but only slightly higher in 1997 and 1998 (5.65 and 6.11 mg g^{-1} for BLcu days and 5.5 and 5.75 mg g^{-1} for clear days). Price and Black (1990) observed a similar effect for a Douglas fir stand on eastern Vancouver Island. Verma et al. (1986), for a deciduous forest in eastern Tennessee during early August 1984, found that WUE averaged between 4 and 7 mg g^{-1} (maximum daily VPD ~ 20 hPa), with higher variability on days with large variations in solar radiation. Differences in WUE for 1996 (8.11 mg g^{-1} for BLcu days vs 5.59 mg g^{-1} for clear days) are likely due to the much greater ET on clear days (11.08 mm day^{-1}), in turn a consequence of more favorable weather [VPD for both clear and BLcu days was virtually the same (~15 hPa)] and abundant soil moisture (~0.25 cm^3 cm^{-3}). The fact that there is little difference in WUE and ET in 1997 and 1998 for both clear and BLcu days may be due to the absence of persistent drought or high temperatures during both growing seasons (see Table 3).

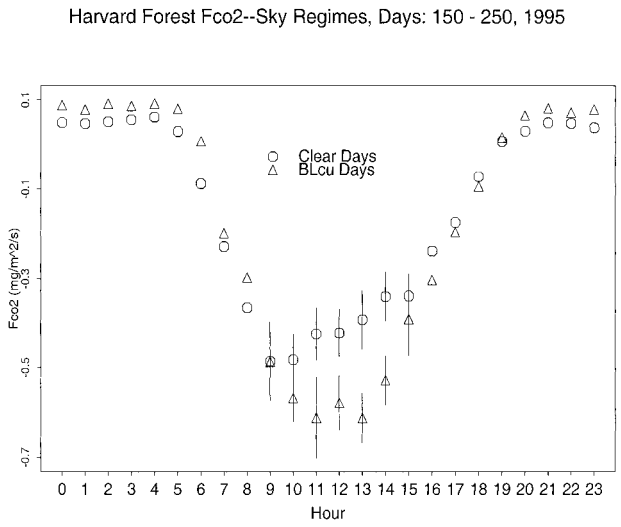

FIG. 13. Diurnal plot of hourly F_{CO_2} (mg m^{-2} s^{-1}) for clear (open circles) and BLcu (open triangles) days at HF, days 150–260, 1995. Vertical lines for hours 0900–1500 LT represent one standard error from the mean.

The impact of environmental stress associated with high VPDs, dry conditions, and lack of clouds throughout the growing season of 1995 is illustrated by diurnal plots of F_{CO_2} on clear and BLcu days (Fig. 13). For clear days, F_{CO_2} peaks during the midmorning (~1000 LT), followed by a gradual decline during the rest of the day. In contrast, on BLcu days, the F_{CO_2} diurnal cycle is almost symmetric, with the peak flux between 1100 and 1300 LT. By midmorning, when the temperature and VPD are rapidly rising, net carbon uptake begins to decrease in response to diurnal and seasonal environmental stresses. These factors were tempered, however, by the presence of BLcu (Fig. 13b).

The 1995 growing season began with a significant drought already under way. The continuing warm and dry conditions may have triggered a feedback mechanism whereby stressed vegetation contributed less moisture than usual to the local environment (apparent from the reduced ET observed during 1995), resulting in higher LCLs and a lower probability of cloud formation. Fewer clouds allowed for higher surface temperatures and greater VPDs, further exacerbating already present environmental stresses, thereby creating a potential positive feedback loop (McNaughton and Jarvis 1991). As previously discussed in section 3a, this may have contributed to the significantly higher LCLs observed during the summer of 1995.

4. Conclusions

a. Findings

1) In the northeastern United States, shortly before the growing season commences, afternoon mixed-layer heights and surface-based LCLs reach their annual maximum, a result of rapidly increasing insolation and higher sensible heat fluxes. With the activation of transpiring vegetation, the change in the energy partition (higher LE and lower H) results in a decrease in z_i (from 1250 to 1100 m) and the LCL (from 1700 to 1500 m), from their early spring maximums. Both z_i and the LCL remain at a nearly constant level on fair days throughout the growing season, as the mixed layer adjusts to its new equilibrium. This thermodynamic transformation of the boundary layer in spring results in a large increase in frequency of BLcu. At ORE, the growing season peak in BLcu frequency is consistent for 1995–98, but its magnitude is somewhat dependent upon longer-term (weeks to months) meteorological conditions, such as drought.
2) BLcu over the eastern United States show a trend toward higher values in time fraction frequency during the growing season, consistent with findings of other land surface–based climatologies. The seasonal trend is dependent upon latitude and topography, similar to other phenological and meteorological indicators of spring (Schwartz 1996; Fitzjarrald et al. 2000). Increases in BLcu frequency first appear in the southeastern states during early spring and reach northern New England by June.
3) Local effects, such as mountain–valley or sea-breeze circulations, are evident when examining diurnal maxima in BLcu time fraction. Upslope flows associated with mountain–valley circulations are likely responsible for the earliest diurnal peaks occurring over mountain stations (around 1300 LT), while valley locations, in response to delayed growth of the mixed layer and subsidence, experience the latest afternoon crests in BLcu frequency (approximately 1500 LT). Sea-breeze effects tend to produce daily maxima in BLcu frequency at about 1330 LT.
4) Light–sky relationships show good linear and quadratic fits when comparing insolation or the standard deviation of insolation at Harvard Forest with sky cover at Orange. A polynomial regression, combining both $K\downarrow$ and std$K\downarrow$ with sky fraction, shows a robust relationship among these variables, despite the ASOS ceilometer's inability to detect clouds above 12 000 ft.
5) Diffuse radiation–cloud cover relationships show a good overall correlation, with absolute maxima in K_{diff} near 0.5 cloud cover.
6) Afternoon net carbon uptake at Harvard Forest under the BLcu sky regime was enhanced during the growing seasons of 1995–98. This was especially evident during 1995, which featured high afternoon VPDs on clear days, persistent drought, and reduced soil moisture. For 1996–98, although temperatures and precipitation were near climatological normals, the BLcu effect was reduced but still significant. Overall, during the growing seasons of 1996–98, BLcu frequency was significantly higher than that observed during 1995. It is likely that the combination of both environmental (higher surface temperatures and VPDs affecting internal carbon fixation in leaves) and physiological (lack of clouds reducing the amount of available diffuse radiation) conditions resulted in the greater reduction of net afternoon carbon uptake observed on clear days during 1995 than in subsequent years.

b. Discussion

Previous studies, focusing mostly on the U.S. Great Plains or the Midwest, are inconclusive with respect to the preferred type of land surface (i.e., cleared vs forested) for BLcu onset and formation. Modeling studies have focused on mesoscale circulations as a favored mechanism for the generation of BLcu (e.g., Segal and Arritt 1992), but observational evidence associating this phenomenon with land surface discontinuities is lacking. Most of the United States, including, with few exceptions, everywhere east of the Mississippi, does not feature land surface contrasts on the scale necessary to generate such circulations. Rabin et al. (1990) suggest that even in areas featuring large-scale patches of adjacent cleared and forested lands (e.g., Oklahoma), BLcu onset and cloud cover are more a function of the surface energy partition than surface type. That BLcu occurrence increases rapidly with the emergence of transpiring vegetation in the eastern United States lends credence to this observation. That the afternoon LCL, RH, and mixed-layer height remain nearly constant throughout the growing season indicates that the coupling between BLcu and the land surface helps maintain the daytime mixed-layer equilibrium.

Given the heterogeneous nature of the land cover in

the eastern United States, observations in section 3b, which relates topographic features and proximity to the ocean or large bodies of water, show that BLcu onset and coverage can be linked to land surface features. However, given the preferred location of surface observing stations (i.e., valleys), the true fractional coverage of BLcu over large areas is likely to be underestimated; satellite observations, given their limited resolution, also underreport BLcu coverage by up to 25%. Since the presence of BLcu is linked with boundary layer exchange processes, including heat, moisture, radiation, and carbon uptake, this has important implications for modeling these processes on short and long timescales. The findings in section 3 relating BLcu onset and coverage to station type could be used to make adjustments to apparent regional BLcu sky cover.

The light–sky relationships derived in section 3c can be used in a wide variety of observational or modeling applications, such as the estimation of surface forcings or potential solar energy availability. Any radiation measurements that include $K\downarrow$ and its standard deviation can be related to general and BLcu sky cover; or sky cover observations can be used to estimate insolation and its standard deviation. Since most solar energy applications rely on estimates of site-specific insolation, sky cover measurements made at standard meteorological observing stations can be converted into insolation estimates from the relationships found in section 3c.

The presence of BLcu provides favorable light and environmental conditions for carbon uptake (see section 3d). During periods of prolonged drought, when temperatures and VPDs are unusually high, and soil moisture is depleted, BLcu furnish temporary relief to stressed vegetation in the form of reduced surface temperatures (and VPD) and provide an additional source of diffuse radiation that penetrates deeper into the forest canopy. Since the occurrence of BLcu is linked with the emergence of deciduous leaves, this coupling of the forested (and actively transpiring) landscape with the appearance of BLcu represents an environmental control that feeds back into mixed-layer (ML) dynamics. An unstressed forest supplies ample moisture (>1 g kg^{-1} day^{-1}) to the ML; this in turn lowers the VPD and the LCL, and facilitates the formation of BLcu. The presence of BLcu further reduces any potential for environmental stresses associated with stomatal closure and reduced C uptake. A steady state is achieved, marked by the almost daily appearance of BLcu during the fair weather days of the growing season. A positive feedback may have been in place during 1995, whereby unusually warm and dry conditions produced higher LCLs, reducing the probability of BLcu formation.

Forest areal coverage in the northeastern United States has increased significantly (from less than 30% to more than 60% of total land surface) since its minimum in the middle 1800s. Previous studies have shown that deforestation leads to decreased ET and rainfall (e.g., Charney 1975), and the presence of large, forested regions can reduce the effect of entrainment drying and increase low-level moisture flux convergence and the probability of precipitation (Fu et al. 1999). It is possible that the reforestation that has occurred in the eastern United States during the past 150 years, accompanied by the concomitant lowering of regional Bowen ratios, may be at least partially responsible for the increase in humidity (Elliot and Angell 1997) and cloudiness (Henderson-Sellers 1989) observed in the United States during the past century.

Acknowledgments. Primary support for this work is from the Joint Program on Terrestrial Ecology and Global Change of the National Aeronautics and Space Administration (NAG 56227) and the Research Foundation of the State University of New York. Flux observations by ASRC at Harvard Forest are supported by the U.S. Department of Energy's (DOE) National Institute for Global Environmental Change (NIGEC) through the NIGEC Northeast Regional Center at Harvard Forest (DOE Cooperative Agreement DE-FC03-90ER61010), under Subcontract 901214 from Harvard University. We are grateful to J. W. Munger and S. C. Wofsy of Harvard University for sharing data and other resources with us. We thank Kathleen Savage of the Woods Hole Research Center for providing us with the soil moisture data referred to in this work. We also appreciate the efforts of personnel at the Albany National Weather Service Forecast Office in providing us with some of the Albany sounding data. We would like to acknowledge the assistance of John Sicker, who provided excellent technical support throughout the term of this study.

REFERENCES

Angström, A., 1924: Solar and terrestrial radiation. *Quart. J. Roy. Meteor. Soc.*, **50,** 121–125.

Anthes, R. A., 1984: Enhancement of convective precipitation by mesoscale variations in vegetative cooling in semiarid regions. *J. Climate Appl. Meteor.*, **23,** 541–554.

Baldocchi, D., 1997: Measuring and modeling carbon dioxide and water vapour exchange over a temperate broad-leaved forest during the 1995 summer drought. *Plant, Cell Environ.*, **20,** 1108–1122.

——, and P. C. Harley, 1995: Scaling carbon dioxide and water vapour exchange from leaf to canopy in a deciduous forest: Model testing and application. *Plant, Cell Environ.*, **18,** 1157–1173.

Benner, T. C., and J. A. Curry, 1998: Characteristics of small tropical cumulus clouds and their impact on the environment. *J. Geophys. Res.*, **103,** 28 753–28 767.

Betts, A. K., 1984: Boundary layer thermodynamics of a high plains severe storm. *Mon. Wea. Rev.*, **112,** 2199–2211.

——, 1985: Mixing line analysis of clouds and cloudy boundary layers. *J. Atmos. Sci.*, **42,** 2751–2763.

Blyth, E. M., A. J. Dolman, and J. Noilhan, 1994: The effect of forest on mesoscale rainfall: An example from HAPEX–MOBILHY. *J. Appl. Meteor.*, **33,** 445–454.

Bradley, J. T., and R. Lewis, 1998: Comparability of ASOS and Human Observations. Preprints, *14th Int. Conf. on Interactive Information and Processing Systems for Meteorology, Oceanography, and Hydrology*, Phoenix, AZ, Amer. Meteor. Soc., 474–478.

Brown, M. E., and D. L. Arnold, 1998: Land–surface–atmosphere

interactions associated with deep convection in Illinois. *Int. J. Climatol.,* **18,** 1637–1653.
Brutsaert, W., and M. Sugita, 1992: Application of self-preservation in the diurnal evolution of the surface energy budget to determine daily evaporation. *J. Geophys. Res.,* **97,** 18 377–18 382.
Bunker, A. F., B. Haurwitz, J. S. Malkus, and H. Stommel, 1949: Vertical distribution of temperature and humidity over the Caribbean Sea. *Pap. Phys. Oceanogr. Meteor.,* **11,** 1–82. Reprint, *Collected Works of Henry M. Stommel,* N. G. Hoggs and R. X. Huang, Eds., Vol. 3, Amer. Meteor. Soc., 1996, 310–368.
Carleton, A., D. Travis, D. Arnold, R. Brinegar, D. E. Jelinski, and D. R. Easterling, 1994: Climatic-scale vegetation–cloud interactions during drought using satellite data. *Int. J. Climatol.,* **14,** 593–623.
Charney, J. G., 1975: Dynamics of deserts and drought in the Sahel. *Quart. J. Roy. Meteor. Soc.,* **101,** 193–202.
Chen, F., and R. Avissar, 1994: Impact of land-surface moisture variability on local shallow convective cumulus and precipitation in large-scale models. *J. Appl. Meteor.,* **33,** 1382–1401.
Clark, C. A., and R. W. Arritt, 1995: Numerical simulations of the effect of soil moisture and vegetation cover on the development of deep convection. *J. Appl. Meteor.,* **34,** 2029–2045.
Cutrim, E., D. W. Martin, and R. Rabin, 1995: Enhancement of cumulus clouds over deforested lands in Amazonia. *Bull. Amer. Meteor. Soc.,* **76,** 1801–1805.
Doran, J. C., W. J. Shaw, and J. M. Hubbe, 1995: Boundary layer characteristics over areas of inhomogeneous surface fluxes. *J. Appl. Meteor.,* **34,** 559–571.
Elliot, W. P., and J. K. Angell, 1997: Variations of cloudiness, precipitable water, and relative humidity over the United States: 1973–1993. *Geophys. Res. Lett.,* **24,** 41–44.
Falconer, R. E., 1948: A method for obtaining a continuous record of the type of clouds in the sky during the day. Final Report, Project Cirrus Rep. RL 140, General Electric Research Laboratory, Schenectady, NY, 135 pp.
——, 1965: A simple method for obtaining a continuous record of the presence and type of clouds in the sky during the day. *Pure Appl. Geophys.,* **60,** 234–244.
Fan, S.-M., and Coauthors, 1995: Environmental controls on the photosynthesis and respiration of a boreal lichen woodland: A growing season of whole-ecosystem exchange measurements by eddy correlation. *Oecologia,* **102,** 443–452.
Fitzjarrald, D. R., and K. E. Moore, 1994: Growing season boundary layer climate and surface exchanges in a subarctic lichen woodland. *J. Geophys. Res.,* **99,** 1899–1917.
——, ——, R. K. Sakai, and J. M. Freedman, 1995: Forest–atmosphere exchange processes: Relationships between leaf state and radiative properties with regional climate, 1991–1995. *Extended Abstracts, Fifth Annual Harvard Forest Ecology Symp.,* Petersham, MA, Harvard Forest Long Term Ecological Research Program, **14,** 598–614.
——, O. C. Acevedo, and K. E. Moore, 2001: Climatic consequences of leaf presence in the eastern United States. *J. Climate,* in press.
Fu, R., B. Zhu, and R. E. Dickinson, 1999: How do atmosphere and land surface influence seasonal changes of convection in the tropical Amazon? *J. Climate,* **12,** 1306–1321.
Gibson, H. M., and T. H. Von der Haar, 1990: Cloud and convection frequencies over the southeast United States as related to small-scale geographic features. *Mon. Wea. Rev.,* **118,** 2215–2227.
Goulden, M. L., J. W. Munger, S.-M. Fan, B. C. Daube, and S. C. Wofsy, 1996: Exchange of carbon dioxide by a deciduous forest: Response to interannual climate variability. *Science,* **271,** 1576–1578.
——, B. C. Daube, S.-M. Fan, D. J. Sutton, A. Bazzaz, J. W. Munger, and S. C. Wofsy, 1997: Physiological responses of a black spruce forest to weather. *J. Geophys. Res.,* **102,** 28 987–28 996.
Henderson-Sellers, A., 1989: North American total cloud amount variations this century. *Global Planet. Change,* **1,** 175–194.
Hollinger, D. Y., F. M. Kelliher, J. N. Byers, J. E. Hunt, T. M. McSeveny, and P. L. Weir, 1994: Carbon dioxide exchange between an undisturbed all-growth temperate forest and the atmosphere. *Ecology,* **75,** 134–150.
Holzworth, G. C., 1964: Estimates of mean maximum mixing depths in the contiguous United States. *Mon. Wea. Rev.,* **92,** 235–242.
——, 1972: *Mixing Heights, Wind Speeds, and Potential for Urban Air Pollution throughout the Contiguous United States.* Environmental Protection Agency, 118 pp.
Jackob, C., 1999: Cloud cover in the ECMWF reanalysis. *J. Climate,* **12,** 947–959.
Jarvis, P. G., R. S. Miranda, and R. I. Meutzelfeldt, 1985: Modeling canopy exchanges of water vapor and carbon dioxide in coniferous forest plantations. *The Forest–Atmosphere Interaction,* B. A. Hutchison and B. B. Hicks, Eds., Reidel, 521–542.
Kimball, H. H., 1919: Variations in total and luminous solar radiation with geographical position in the United States. *Mon. Wea. Rev.,* **47,** 780.
——, 1928: Amount of solar radiation that reaches the surface of the earth on the land and on the sea, and methods by which it is measured. *Mon. Wea. Rev.,* **56,** 393–398.
Lynn, B. H., W.-K. Tao, and P. J. Wetzel, 1998: A study of landscape-generated deep moist convection. *Mon. Wea. Rev.,* **126,** 928–942.
Mahfouf, J. F., E. Richard, and P. Mascart, 1987: The influence of soil and vegetation on the development of mesoscale circulations. *J. Climate Appl. Meteor.,* **26,** 1483–1494.
Mahrt, L., J. Sun, D. Vickers, J. I. MacPherson, J. R. Pederson, and R. L. Desjardins, 1994: Observations of fluxes and inland breezes over a heterogeneous surface. *J. Atmos. Sci.,* **51,** 2484–2499.
Marotz, G. A., J. Clark, J. Henry, and R. Standfast, 1975: Cloud fields over irrigated areas in southwestern Kansas—Data and speculations. *Prof. Geogr.,* **27,** 457–461.
McNaughton, K. G., and P. G. Jarvis, 1991: Effects of spatial scale on stomatal control of transpiration. *Agric. For. Meteor.,* **54,** 279–301.
Monteith, J. L., 1995: Accommodation between transpiring vegetation and the convective boundary layer. *J. Hydrol.,* **166,** 251–263.
——, and M. Unsworth, 1990: *Principles of Environmental Physics.* 2d ed. Edward Arnold, 290 pp.
Moore, K. E., D. R. Fitzjarrald, R. K. Sakai, M. L. Goulden, J. W. Munger, and S. C. Wofsy, 1996: Seasonal variations in radiative and turbulent exchange at a deciduous forest in central Massachusetts. *J. Appl. Meteor.,* **35,** 122–134.
Munger, J. W., and Coauthors, 1996: Atmospheric deposition of nitrogen oxides and ozone in a temperate deciduous forest and a sub-arctic woodland. I. Measurements and mechanisms. *J. Geophys. Res.,* **101,** 12 639–12 675.
NCDC, 1998: *NCDC Summary of the Day.* EarthInfo, Inc., CD-ROM.
NOAA, 1998: ASOS user's guide. National Oceanographic and Atmospheric Administration, 61 pp. [Available online at http://www.nws.noaa.gov/asos.]
O'Neal, M., 1996: Interactions between land cover and convective cloud cover over midwestern North America detected from GOES satellite data. *Int. J. Remote Sens.,* **17,** 1149–1181.
Paluch, I. R., 1979: The entrainment mechanism in Colorado cumuli. *J. Atmos. Sci.,* **36,** 2467–2478.
Pochop, L. O., M. D. Shanklin, and D. A. Horner, 1968: Sky cover influence on total hemispheric radiation during daylight hours. *J. Appl. Meteor.,* **7,** 484–489.
Prescott, J. A., 1940: Evaporation from a water surface in relation to solar radiation. *Trans. Roy. Soc. South Aust.,* **64,** 114–125.
Price, D. T., and T. A. Black, 1990: Effects of short-term variation in weather on diurnal canopy CO_2 flux and evapotranspiration of a juvenile Douglas-fir stand. *Agric. For. Meteor.,* **50,** 139–158.
Rabin, R. M., and D. W. Martin, 1996: Satellite observations of shallow cumulus coverage over the central United States: An exploration of land use impact on cloud cover. *J. Geophys. Res.,* **101,** 7149–7155.
——, S. Stadler, P. J. Wetzel, D. J. Stensrud, and M. Gregory, 1990:

Observed effects of landscape variability on convective clouds. *Bull. Amer. Meteor. Soc.,* **71,** 272–280.
Richardson, L. F., 1922: *Weather Prediction by Numerical Processes.* Cambridge University Press, Reprint, Dover, 1965.
Rossow, W. B., and R. A. Schiffer, 1991: ISCCP cloud data products. *Bull. Amer. Meteor. Soc.,* **72,** 2–20.
——, A. W. Walker, and L. C. Garder, 1993: Comparison of ISCCP and other cloud amounts. *J. Climate,* **6,** 2394–2418.
Ruimy, A., P. G. Jarvis, D. D. Baldocchi, and B. Saugier, 1995: CO_2 fluxes over plant canopies and solar radiation: A literature review. *Adv. Ecol. Res.,* **26,** 1–68.
Sakai, R. K., D. R. Fitzjarrald, and K. E. Moore, 1997: Detecting leaf area and surface resistance during transition seasons. *Agric. For. Meteor.,* **84,** 273–284.
Savage, K., E. Davidson, and E. Belk, 1998: Interannual variation in soil respiration rates at Harvard Forest. *Extended Abstracts, Ninth Annual Harvard Forest Ecology Symp.,* Petersham, MA, Harvard Forest Long Term Ecological Research Program,43–44.
Schwartz, M. D., 1996: Examining the spring discontinuity in daily temperature ranges. *J. Climate,* **9,** 803–808.
Segal, M., and R. W. Arritt, 1992: Nonclassical mesoscale circulations caused by surface sensible heat-flux gradients. *Bull. Amer. Meteor. Soc.,* **73,** 1593–1604.
——, M. Leuthold, R. W. Arritt, C. Anderson, and J. Shen, 1997: Small lake daytime breezes: Some observational and conceptual evaluations. *Bull. Amer. Meteor. Soc.,* **78,** 1135–1147.
Shuttleworth, W. J., 1991: Insight from large-scale observational studies of land/atmosphere interactions. *Surv. Geophys.,* **12,** 3–30.
Stommel, H., 1947: Entrainment of air into a cumulus cloud. *J. Meteor.,* **4,** 91–94.
Stull, R. B., 1988: *An Introduction to Boundary Layer Meteorology.* Kluwer, 666 pp.
——, 1992: Impact of boundary-layer clouds—A case study of cover hours. *J. Climate,* **5,** 390–394.
Tiedtke, M., 1989: A comprehensive mass-flux scheme for cumulus parameterization in large-scale models. *Mon. Wea. Rev.,* **117,** 1779–1800.
——, 1993: Representation of clouds in large-scale models. *Mon. Wea. Rev.,* **121,** 3040–3051.
Trenberth, K. E., 1999: Atmospheric moisture recycling: Role of advection and local evaporation. *J. Climate,* **12,** 1368–1381.
Verma, S. B., D. D. Baldocchi, D. E. Anderson, D. R. Matt, and R. J. Clement, 1986: Eddy fluxes of CO_2, water vapor, and sensible heat over a deciduous forest. *Bound.-Layer Meteor.,* **36,** 71–91.
Warren, S., C. Hahn, J. London, R. Chervin, and R. Jenne, 1986: Global distribution of total cloud cover and cloud type amounts over land. NCAR Tech. Note TN-273+STR, 229 pp.
Weare, B. C., I. I. Mokhov, and Project Members, 1995: Evaluation of total cloudiness and its variability in the Atmospheric Model Intercomparison Project. *J. Climate,* **8,** 2224–2238.
Wielicki, B. A., and R. M. Welch, 1986: Cumulus cloud properties derived using Landsat satellite data. *J. Climate Appl. Meteor.,* **25,** 261–276.
Wofsy, S. C., M. L. Goulden, J. W. Munger, S.-M. Fan, P. S. Bakwin, B. C. Daube, S. L. Bassow, and F. A. Bazzaz, 1993: Net exchange of CO_2 in midlatitude forests. *Science,* **260,** 1314–1317.
Woodcock, D. W., 1992: The rain on the plain: Are there vegetation–climate feedbacks? *Global Planet. Change,* **5,** 191–202.
World Meteorological Organization, 1969: *WMO International Cloud Atlas* (abridged). WMO, 62 pp. and 72 plates.
Zhong, S., and J. C. Doran, 1997: A study of the effects of spatially varying fluxes on cloud formation and boundary layer properties using data from the Southern Great Plains Cloud and Radiation Testbed. *J. Climate,* **10,** 327–341.